NeuroImage 69 (2013) 213–222

Contents lists available at SciVerse ScienceDirect

NeuroImage

journal homepage: www.elsevier.com/locate/ynimg

KIBRA gene variants are associated with synchronization within the default-mode and executive control networks

Dawei Wang [a,1], Bing Liu [b,1], Wen Qin [a,1], Junping Wang [a], Yunting Zhang [a], Tianzi Jiang [b,*], Chunshui Yu [a,c,**]

[a] Department of Radiology, Tianjin Medical University General Hospital, Tianjin 300052, China
[b] LIAMA Center for Computational Medicine, National Laboratory of Pattern Recognition Institute of Automation, Chinese Academy of Sciences, Beijing 100190, China
[c] School of Medical Imaging, Tianjin Medical University, Tianjin 300052, China

ARTICLE INFO

Article history:
Accepted 13 December 2012
Available online 22 December 2012

Keywords:
KIBRA
Episodic memory
Executive function
Resting state network
MRI

ABSTRACT

Genetic variation at the KIBRA rs17070145 polymorphism has been linked to episodic memory, executive function, and Alzheimer's disease (AD), which are related to the structural and functional integrity of the default-mode network (DMN) and executive control network (ECN). We hypothesize that the KIBRA polymorphism could modulate the structure and function of the DMN and ECN in healthy young subjects, which might underlie the association between this gene and cognitive function. To test our hypothesis, we analyzed the resting-state synchronization in the DMN and ECN in 288 young, healthy Chinese Han subjects. We found that carriers of the KIBRA C-allele demonstrated an increased synchronization in the posterior cingulate cortex (PCC) and medial prefrontal cortex (MPFC) of the DMN and in the right anterior insula, bilateral caudate nuclei, and bilateral dorsal anterior cingulate cortices (dACC) of the ECN compared to individuals with a TT genotype. Moreover, KIBRA C-allele carriers also showed a smaller gray matter volume (GMV) in the MPFC and bilateral dACCs than TT individuals. In contrast, there were no significant genotype differences in the synchronization of either the visual network or the sensorimotor network. These findings suggest that the polymorphism in the KIBRA gene affects GMV and the function of the DMN and ECN. This increased synchronization is likely a reflection of compensation for the regional gray matter deficits in these networks in young healthy subjects. The association between KIBRA polymorphisms and the DMN and ECN should be further explored in a healthy older population and in patients with AD.

Introduction

The neural mechanisms underlying the association between the polymorphism in the KIBRA gene and cognitive function remain largely undefined. A common rs17070145 polymorphism in the KIBRA gene has been associated with episodic memory (Almeida et al., 2008; Bates et al., 2009; Kauppi et al., 2011; Papassotiropoulos et al., 2006; Preuschhof et al., 2010; Schaper et al., 2008; Vassos et al., 2010; Yasuda et al., 2010) and executive function (Wersching et al., 2011; Zhang et al., 2009a) in healthy subjects and has also been linked to the risk for late-onset Alzheimer's disease (AD) (Beecham et al., 2009; Burgess et al., 2011; Corneveaux et al., 2010; Rodriguez-Rodriguez et al., 2009). Only three studies have investigated the neural mechanisms of the polymorphism in the KIBRA gene and two of these studies focused on hippocampal activation (Kauppi et al., 2011; Papassotiropoulos et al., 2006). The present study aimed to test the hypothesis that the polymorphism in the KIBRA gene specifically affects cognitive-related functional networks.

The association between the polymorphism in the KIBRA gene and episodic memory has been extensively investigated (Table S1). Most of these studies showed a beneficial effect of the T-allele on episodic memory (Almeida et al., 2008; Bates et al., 2009; Kauppi et al., 2011; Papassotiropoulos et al., 2006; Preuschhof et al., 2010; Schaper et al., 2008; Vassos et al., 2010; Yasuda et al., 2010), although non-significant (Bates et al., 2009; Burgess et al., 2011; Jacobsen et al., 2009; Need et al., 2008; Wersching et al., 2011) and deleterious effects (Nacmias et al., 2008; Wagner et al., 2012) have also been demonstrated. As for executive functions (Table S2), a non-significant association has commonly been reported (Nacmias et al., 2008; Papassotiropoulos et al., 2006; Preuschhof et al., 2010; Schaper et al., 2008; Wagner et al., 2012; Zhang et al., 2009a); however, two studies found a significant association (Wersching et al., 2011; Zhang et al., 2009a). The KIBRA C-allele homozygote is frequently associated with an increased risk for AD (Burgess et al., 2011; Corneveaux et al., 2010), although negative (Hayashi et al.,

* Correspondence to: T. Jiang, LIAMA Center for Computational Medicine, National Laboratory of Pattern Recognition, Institute of Automation, Chinese Academy of Sciences, Beijing 100190, China. Fax: +86 10 6255 1993.
** Correspondence to: C. Yu, Department of Radiology, Tianjin Medical University General Hospital, No. 154, Anshan Road, Heping District, Tianjin 300052, China. Fax: +86 2263062290.
E-mail addresses: jiangtz@nlpr.ia.ac.cn (T. Jiang), chunshuiyu@yahoo.cn (C. Yu).
[1] D.W., B.L., and W.Q. contributed equally to this work.

1053-8119/$ – see front matter © 2013 Elsevier Inc. All rights reserved.
http://dx.doi.org/10.1016/j.neuroimage.2012.12.022

2010) and contradictory findings (Rodriguez-Rodriguez et al., 2009) have also been reported (Table S3).

The effects of the polymorphism in the KIBRA gene on brain functions have been investigated in three functional neuroimaging studies. Two functional MRI studies focused on the activation of the hippocampus during memory retrieval in healthy individuals and reported increased activation in young CC carriers (Papassotiropoulos et al., 2006) or in old T-allele carriers (Kauppi et al., 2011). A positron emission tomography (PET) study revealed lower resting-state glucose metabolism in KIBRA T-allele non-carriers relative to carriers in the posterior cingulate cortex and precuneus (PCC/Pcu) (Corneveaux et al., 2010).

It is generally accepted that a specific cognitive function is controlled by a distributed neuronal network rather than a brain region. For example, episodic memory is associated with the default-mode network (DMN) (Daselaar et al., 2004; Greicius et al., 2004; Otten and Rugg, 2001; Wagner et al., 2005; Wheeler and Buckner, 2003), whereas executive function is controlled by the executive control network (ECN) (Beckmann et al., 2005; Fox et al., 2006; Greicius et al., 2003; Roosendaal et al., 2010; Seeley et al., 2007).

The DMN is mainly composed of the PCC/Pcu, the medial prefrontal and anterior cingulate cortices (MPFC/ACC), and the bilateral inferior parietal cortices (IPC) (Buckner et al., 2008; Fox et al., 2005; Greicius et al., 2004; Raichle et al., 2001). This network is deactivated during cognitively demanding tasks and shows increased activity during resting-state and self-referential tasks (Buckner et al., 2008; Schacter et al., 2007; Spreng et al., 2009; Svoboda et al., 2006). In patients with AD, both the structural and functional deficits have been frequently reported in areas within the DMN (Greicius et al., 2004; Sorg et al., 2007; Wang et al., 2007; Zhang et al., 2009b). Even in cognitively normal participants, the ε4 allele of apolipoprotein E (APOE4), the major genetic susceptibility factor for late-onset AD, has a substantial influence on the functional characteristics of the DMN (Filippini et al., 2009). If the KIBRA polymorphism is associated with episodic memory and AD, we hypothesize that this gene may also affect the structure and function of the DMN, even in healthy young subjects. Indeed, two pieces of evidence have suggested that the functional characteristics of the DMN are affected by the polymorphism in the KIBRA gene. One study of healthy young subjects reported that CC-carriers showed increased activation in the MPFC during an associative episodic memory task compared with T-allele (TT + CT) carriers (Papassotiropoulos et al., 2006). In cognitively normal, late-middle-aged individuals, KIBRA CC-carriers exhibited lower glucose metabolism in the PCC/Pcu, compared to T-allele carriers (Corneveaux et al., 2010). However, it remains unclear how the polymorphism of the KIBRA gene modulates the resting-state synchronization of the DMN and how the structural and functional characteristics of the DMN affect each other. Moreover, the effect of the polymorphism of the KIBRA gene on the ECN has never been investigated.

Here, we used a multimodal neuroimaging approach to investigate the structural and functional characteristics of the DMN and ECN in 121 KIBRA C-allele carriers and 167 KIBRA TT-individuals, with ages ranging from 20 to 33 years old. Our first aim was to test the differences in synchronization within the DMN and ECN between the two genotype groups using resting-state functional MRI. Then, we further investigated whether the gray matter volumes (GMV) of the DMN and ECN regions with significant differences in synchronization differed between the two genotype groups.

Materials and methods

Subjects

A total of 288 healthy, young, right-handed subjects (mean age: 22.7 ± 2.5 years; 133 males) were selected from 323 subjects who participated in this study after giving written informed consent, in accordance with the local Medical Research Ethics Committee of Tianjin Medical University. Thirty-five subjects were excluded from further analysis due to a lack of genetic data or excessive head movement during the fMRI examinations. Careful screening was performed to ensure that all participants were free of any lifetime history of psychiatric or neurological illness, psychiatric treatment, or drug or alcohol abuse, and MR contraindications. To avoid population stratification artifacts, only Chinese Han subjects were included. Memory function was assessed by the Chinese Revised Wechsler Memory Scale (WMS-RC) (Gong, 1989) and executive function was assessed by the Wisconsin Card Sorting Test (WCST) (Heaton, 1999). In addition, 9 subjects were excluded from the analysis of the WMS-RC and one was excluded from the analysis of the WCST due to the lack of behavioral data.

Genotyping

We extracted genomic DNA from 3000 μL of whole blood using the EZgeneTM Blood gDNA Miniprep Kit (Biomiga Inc., San Diego, CA, USA). Then, we genotyped the KIBRA rs17070145 in each subject using the PCR and ligation detection reaction (LDR) method (Thomas et al., 2004; Yi et al., 2009) with technical support from the Shanghai Biowing Applied Biotechnology Company.

The PCR primer sequences were as follows: forward: 5′ CACTG GGGACCCACATTTAC 3′, reverse 5′ CACAATGAACAAGGCTGTGG 3′. PCR was carried out in 20 μL volume containing 1 μL genomic DNA, 0.4 μL primer mixture, 2 μL dNTPs, 0.6 μL Mg^{2+}, 2 μL buffer, 4 μL Q-Solution, and 0.3 μL Taq DNA polymerase. The amplification protocol consisted of an initial denaturation and enzyme activation phase at 95 °C for 15 min followed by 35 cycles of denaturation at 94 °C for 30 s, annealing at 59 °C for 1 min and 30 s, extension at 72 °C for 1 min, and then a final extension at 72 °C for 7 min. PCR products were verified in 3% agarose gels that had been stained with ethidium bromide to regulate the amount of DNA added to the LDR.

Three probes were designed for the LDR reactions, including one common probe (rs17070145_modify: P-AGGTCCAGGATCAAGGAGCA GCTGGTTTTTTTTTTTTTTT-FAM) and two discriminating probes for the two alleles (rs17070145_C: TTTTTTTTTTTTTTTTAAAAGGAAAGC TCAGGAACAGTTG; rs17070145_T: TTTTTTTTTTTTTTTTTTAAAAGGAA AGCTCAGGAACAGTTA). These reactions were carried out in a 10 μL mixture containing 1 μL buffer, 1 μL probe mix, 0.05 μL Taq DNA ligase, 1 μL PCR product, and 6.95 μL deionized water. The reaction program consisted of an initial heating at 95 °C for 2 min followed by 35 cycles of 30 s at 94 °C and 2 min at 50 °C. Reactions were stopped by chilling the tubes in an ethanol–dry ice bath and adding 0.5 mL of 0.5 mM EDTA. Aliquots of 1 μL of the reaction products were mixed with 1 μL of loading buffer (83% formamide, 8.3 mM EDTA and 0.17% blue dextran) and 1 μL ABI GS-500 Rox-Fluorescent molecular weight marker, denatured at 95 °C for 2 min, and chilled rapidly on ice prior to being loaded on an 5 M urea–5% polyacrylamide gel and electrophoresed on an ABI 3100 DNA sequencer at 3000 V. Finally fluorescent ligation products were analyzed and quantified using the ABI GeneMapper software.

Image acquisition

MR images were acquired using a Signa HDx 3.0 Tesla MR scanner (General Electric, Milwaukee, WI, USA). Tight but comfortable foam padding was used to minimize head movement, and earplugs were used to reduce scanner noise. Resting-state fMRI data were obtained using Gradient-Echo Single-Shot Echo-Planar Imaging sequence (GRE-SS-EPI) with the following imaging parameters: repetition time (TR)/echo time (TE) = 2000/30 ms; field of view (FOV) = 240 mm × 240 mm; matrix = 64 × 64; flip angle (FA) = 90°; slice thickness = 4 mm; no gap; 40 transversal slices; and 180 volumes. During the fMRI scans, all subjects were instructed to keep their eyes closed, to stay as still as possible, to think of nothing in particular, and to not fall asleep. Sagittal 3D T1-weighted images were

acquired by a brain volume (BRAVO) sequence (TR/TE = 8.1/3.1 ms; inversion time = 450 ms; FA = 13°; FOV = 256 mm × 256 mm; matrix = 256 × 256; slice thickness = 1 mm, no gap; 176 slices).

fMRI data preprocessing

The fMRI data were preprocessed using the Statistical Parametric Mapping (SPM8, http://www.fil.ion.ucl.ac.uk/spm) and Data Processing Assistant for Resting-State fMRI (DPARSF) (Chao-Gan and Yu-Feng, 2010). The first 10 volumes of each functional time series were discarded due to the signal reaching equilibrium and the participants adapting to the scanning noise. The remaining 170 volumes were corrected for the acquisition time delay between different slices and were realigned to the first volume. Head movement parameters were computed by estimating the translation in each direction and the angular rotation on each axis for each volume. Overall, 17 subjects out of 323 were excluded from further analysis because they had a maximum displacement in one or more of the orthogonal directions > 2 mm or a maximum rotation > 2.0°. Following this step, the individual structural images (high-resolution T1-weighted images) were co-registered to the mean functional image after the motion was corrected with a linear transformation (Collignon et al., 1995). The transformed structural images were then segmented into gray matter (GM), white matter and cerebrospinal fluid using a unified segmentation algorithm (Ashburner and Friston, 2005). The movement-corrected functional volumes were spatially normalized to the Montreal Neurological Institute (MNI) space and re-sampled to 2-mm^3 voxels using the normalization parameters estimated during the unified segmentation. The normalized fMRI data were smoothed with 4 mm full width at half maximum (FWHM).

Independent component analysis (ICA)

We performed the ICA by using the group ICA (GICA) program of the fMRI toolbox (Stable and Consistent Group ICA of fMRI Toolbox, version 1.2; http://www.nitrc.org/projects/cogicat/) established for the analysis of fMRI data. Recently, Zhang et al. (2010) found that in multi-stage principal component analysis (PCA) reduction which is adopted and implemented in GIFT (Calhoun et al., 2001) and MELODIC (Smith et al., 2004), different subject concatenation orders (SCOs) produce variations in GICA results. To achieve robust and accurate results, an improved algorithm, Subject order independent group ICA (SOI-GICA), was implemented, each time with a randomized initial value and a different subject order. The results of multiple runs were then integrated to obtain the final output. The fMRI toolbox supports a GICA approach, which first concatenates the individual data across time, and then computes the subject-specific components and time courses. The fMRI toolbox performed the analysis in three stages: (*i*) data reduction, (ii) application of the ICA algorithm, and (iii) back-reconstruction for each individual subject. In the present study, we adopted the SOI-GICA, performed GICA 100 times and obtained 20 independent components (ICs). Five meaningful components were identified by visual inspection, including the anterior DMN (aDMN), posterior DMN (pDMN), executive control network (ECN), sensorimotor network (SMN) and visual network (VN). The individual-level components were obtained from back-reconstruction and converted into z-scores.

Independent component patterns representing resting state networks (RSNs) were entered into a random-effect one-sample *t*-test. We used $t > 15$ to select voxels of a component to improve the representation of each brain network. A two-sample *t*-test was used to compare the synchronization differences within each network between the two genotype groups with gender, age and education duration as nuisance covariates. A correction for multiple comparisons was performed using a Monte Carlo simulation, resulting in a corrected threshold of $P < 0.05$ (AlphaSim program in AFNI software, http://afni.nimh.nih.gov/. Parameters: single voxel $P = 0.01$, 5000 simulations, FWHM = 4 mm, cluster connection radius r = 3.5 mm; with a gray matter mask and a resolution of 2 mm × 2 mm × 2 mm, http://afni.nimh.nih.gov/).

GMV analysis

The GMV analysis was performed using SPM8 (http://www.fil.ion.ucl.ac.uk/spm/software/spm8). The structural MR images were segmented into GM, white matter and cerebrospinal fluid using the standard unified segmentation model in SPM8. Following segmentation, GM population templates were generated from the entire image dataset using the diffeomorphic anatomical registration through the exponentiated Lie algebra (DARTEL) technique (Ashburner, 2007). After an initial affine registration of the GM DARTEL template to the tissue probability map in MNI space (http://www.mni.mcgill.ca/), nonlinear warping of GM images was performed to the DARTEL GM template in MNI space with a resolution of 1.5-mm^3 (as recommended for the DARTEL procedure). The GMV of each voxel was obtained by multiplying the GM concentration map by the non-linear determinants derived from the spatial normalization step. Finally, to compensate for residual between-subject anatomical differences, the GMV images were smoothed with a full width at half maximum (FWHM) kernel of 8 mm. In effect, here the regional GMV represents normalized GMV after removing the confounding effect of variance in individual brain sizes. After these processing steps, the smoothed, modulated, and normalized GMV maps were used for statistical analysis.

Region of interest (ROI)-based analysis was used to test the GMV difference between the two genotypes. These ROIs were defined as the brain areas that showed significant differences in synchronization between the two genotypes. Thus, seven ROIs were identified and extracted. Inter-group GMV difference of each ROI was compared using a two-sample *t*-test with a threshold of $P < 0.05$ controlled for gender, age and years of education.

A voxel-based exploratory GMV comparison between the two genotype groups was also performed throughout the whole brain using two-sample *t*-test controlled for gender, age and years of education. A loose threshold of $P < 0.01$ (uncorrected) and a cluster threshold of > 200 voxels were adopted.

Statistical analyses of demographic and behavioral data

The demographic and behavioral data were analyzed using the Statistical Package for the Social Sciences version 16.0 (SPSS, Chicago, IL, USA). Group comparisons of these data were performed using a χ^2 test for categorical variables and *t*-tests for continuous variables.

Results

Participants

A total of 288 healthy young Chinese Han subjects with high-quality imaging data and KIBRA genotype information were included in the current study. According to the KIBRA genotypes, these subjects were divided into two groups of 121 C-allele carriers (including 14 CC and 107 CT carriers) and 167 TT homozygotes. This grouping method is consistent with a previous study of Japanese patients with AD (Hayashi et al., 2010), but is inconsistent with most previous KIBRA studies in which the CT and TT carriers were combined into T-allele carriers. The genotype distribution of the SNP was in Hardy–Weinberg equilibrium [$\chi^2(2) = 0.36$, $P = 0.55$]. There were no significant differences ($P > 0.05$) in age, gender, years of education, memory and WCST scores between the two genotype groups (Tables 1 and 2); however, the CC group showed a trend towards decreased memory and executive function (Fig. S1).

Network components

SOI-GICA identified 20 ICs representing group-averaged networks of brain regions with temporally correlated fMRI signals (Beckmann and Smith, 2005; Beckmann et al., 2005; Beckmann et al., 2009; Damoiseaux et al., 2006; De Luca et al., 2006; Mantini et al., 2007). Two ICs were identified as the DMN. One was the aDMN, which was mainly composed of the MPFC and the ACC (Fig. 1A), and the other was the pDMN, which mainly consisted of the PCC/Pcu and the bilateral IPC (Fig. 1B). The ECN included the dorsolateral prefrontal cortex (DLPFC), dorsal anterior cingulate cortex (dACC), caudate nuclei (Cau), and anterior insula (AI) (Beckmann et al., 2005; Fox et al., 2006; Greicius et al., 2003; Seeley et al., 2007) (Fig. 1C). The SMN included the bilateral precentral gyri, postcentral gyri, and supplementary motor areas (Fig. 1D). The VN consisted predominantly of the visual cortex (Fig. 1E).

Synchronization differences in brain networks between KIBRA genotypes

Synchronization in the DMN was compared between individuals with KIBRA TT homozygotes and C-allele carriers. Compared with TT homozygotes, KIBRA C-allele carriers showed significantly ($P<0.05$, corrected) increased synchronization in the right MPFC of the aDMN (peak MNI coordinates: x = 4, y = 62, z = 16) and in the left PCC of the pDMN (x = −10, y = −54, z = 26) (Fig. 2). No brain regions in the C-allele carriers showed significantly decreased synchronization in the DMN compared to TT homozygotes. Within the ECN, KIBRA C-allele carriers showed significantly ($P<0.05$, corrected) increased synchronization in the right AI (x = 34, y = 12, z = 0), bilateral Cau (left: x = −12, y = 6, z = 10;right: x = 16, y = 18, z = 4), and bilateral dACC (left: x = −2, y = 22, z = 38; right: x = 8, y = 16, z = 36) (Fig. 2); no significant decline in synchronization was found within the ECN in the C-allele carriers compared to TT individuals ($P<0.05$, corrected). In contrast to synchronization differences in the DMN and ECN, there were no significant differences ($P<0.05$, corrected) in synchronization in either the SMN or the VN between the two genotypes. These findings suggest that the polymorphism in the KIBRA gene specifically affects the functional synchronization in the DMN and ECN.

We further tested differences in network synchronization among the CC, CT and TT groups, because our grouping method is different from most previous studies. First, we investigated the main effect of the KIBRA genotype on the network synchronization among the three groups (CC: n = 14; CT: n = 107; TT: n = 167) using analysis of variance (ANOVA) after controlling for age, gender, and years of education with a threshold of $P<0.05$ (uncorrected) and a cluster size of >100 voxels. We found significant main effects of the KIBRA genotype in the right MPFC of the aDMN, left PCC of the pDMN, right AI, bilateral Cau, and bilateral dACC of the ECN (Fig. S2). Then, we defined the seven significant brain regions as ROIs and extracted their synchronization indices for further analysis. A permutation method was run 5000 times on the data for 14 subjects from each of the three groups. For each permutation, the synchronization indices of the 7 ROIs were compared between every pair of the three groups ($P<0.05$). For each ROI, the percentage of permutations with a significant difference ($P<0.05$) was computed and is shown in Fig. 3. If we used 15% as a threshold of a trend of significance, we found that three (the right dACC, left Cau, and right Cau) of the seven ROIs showed an allele-dependent effect (CC > CT > TT) in synchronization. For the other four ROIs (the MPFC, PCC, right AI, and left dACC), the synchronization indices of the CT group differed from those of the TT group (>30%), but did not differ from those of the CC group (<5%). These findings suggest that the combination of the CC and CT is more reasonable. Moreover, we also applied a leave-one-out method to extract subjects (CC: n = 13; CT: n = 106; TT: n = 166) from each genotype group (CC: n = 14; CT: n = 107; TT: n = 167) 5000 times. For each leave-one-out, synchronization indices of the 7 ROIs were compared between every pair of the three groups ($P<0.05$). For each ROI, the percentage of tests with significant differences ($P<0.05$) was computed and is shown in parentheses in Fig. 3. We again found that three (the right dACC, left Cau, and right Cau) of the seven ROIs showed an allele-dependent effect (CC > CT > TT) in synchronization indices. For the other four ROIs (the MPFC, PCC, right AI, and left dACC), synchronization indices of the CT group differed from the TT group (100%), but these indices did not differ from the CC group (0%). These findings further suggest that the combination of the CC and CT is more reasonable.

To further validate our findings, a paired *t*-test was also used to compare the differences in synchronization in the seven ROIs between every pair of the three groups (14 subjects per group), matched for gender, age, and years of education (Table S4). We found that the results were similar with the above analyses (Fig. S3).

Table 1
Demographic data of subjects with memory scores.

	CC + CT	TT	*P* value
Number of subjects	118	161	
Age (years)	22.9 (2.5)	22.7 (2.4)	0.47
Sex (male/female)	55/63	74/87	0.92
Years of education	15.8 (2.4)	15.6 (1.9)	0.38
MQ	114.8 (9.4)	115.2 (9.6)	0.69

The data are shown as the means (SD). *MQ*, Memory Quotient.

Table 2
Demographic data of subjects with executive function scores.

	CC + CT	TT	*P* value
Number of subjects	121	166	
Age (years)	22.8 (2.6)	22.8 (2.5)	0.98
Years of education	15.8 (2.4)	15.6 (1.9)	0.63
Sex (male/female)	58/63	75/91	0.64
WSCT indices			
Rpe%	16.9 (0.8)	15.6 (0.7)	0.24

The data are shown as the means (SD). *Rpe%*, percentage of perseverative errors; and WCST, Wisconsin Card Sorting Test.

GMV differences in DMN and ECN between KIBRA genotypes

Based on the SOI-GICA analysis, we found two brain regions in the DMN and five regions in the ECN with significant synchronization differences between the two genotype groups. We wanted to know whether these regions also showed GMV differences across genotypes. The answer to this question would help determine the role of the functional synchronization differences between the two genotypes. We compared the GMV of brain regions that had a significant synchronization difference between the two genotypes. We found that C-allele carriers showed a significant decrease in GMV in the right MPFC ($P = 0.03$) of the aDMN and in the left ($P = 0.004$) and right dACC ($P = 0.018$) of the ECN compared to individuals with the TT genotype (Fig. 4).

We also performed a whole-brain voxel-based analysis using a loose threshold of $P<0.01$ (uncorrected) and found that the C-allele carriers showed significantly lower regional GMV than the TT carriers in the frontal, parietal, and temporal lobes, including most brain regions found in ROI-based analysis (Fig. S4 and Table S5). We did not find any regions with increased GMV in the C-allele carriers compared to the TT subjects.

White matter volume and integrity between KIBRA genotypes

We also analyzed white matter volume using the VBM analysis of structural MRI data and studied white matter integrity using

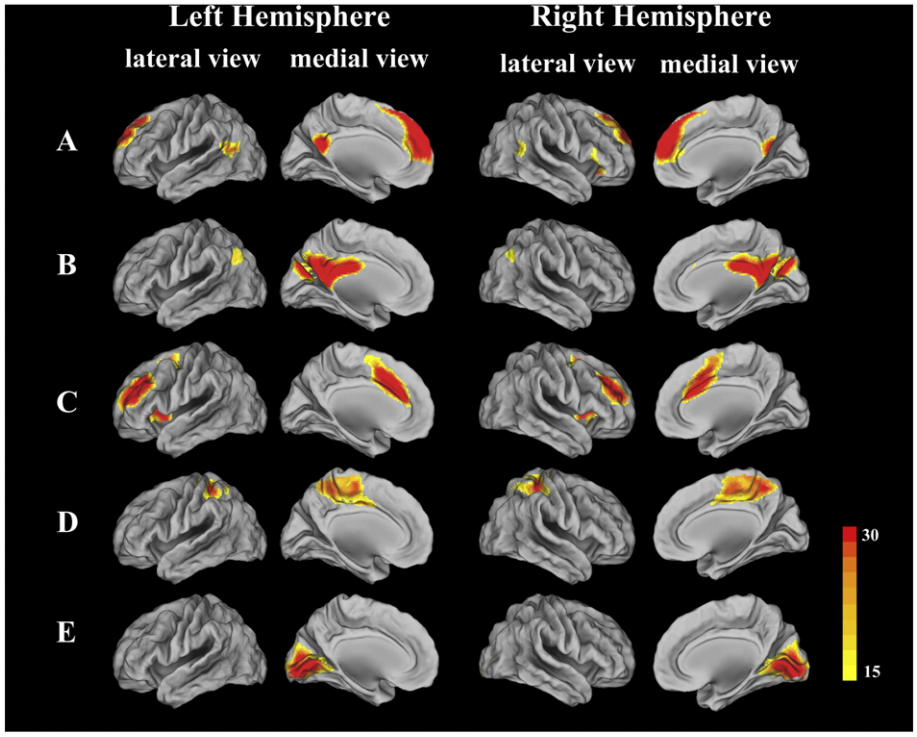

Fig. 1. Cortical representation of brain networks identified in an independent component analysis. (A) Anterior default-mode network (aDMN); (B) Posterior default-mode network (pDMN); (C) Executive control network (ECN); (D) Sensorimotor network (SMN); and (E) Visual network (VN). Color bar represents the *t*-values ranging from 15 to 30. Data are displayed on the lateral, medial surfaces of each hemisphere.

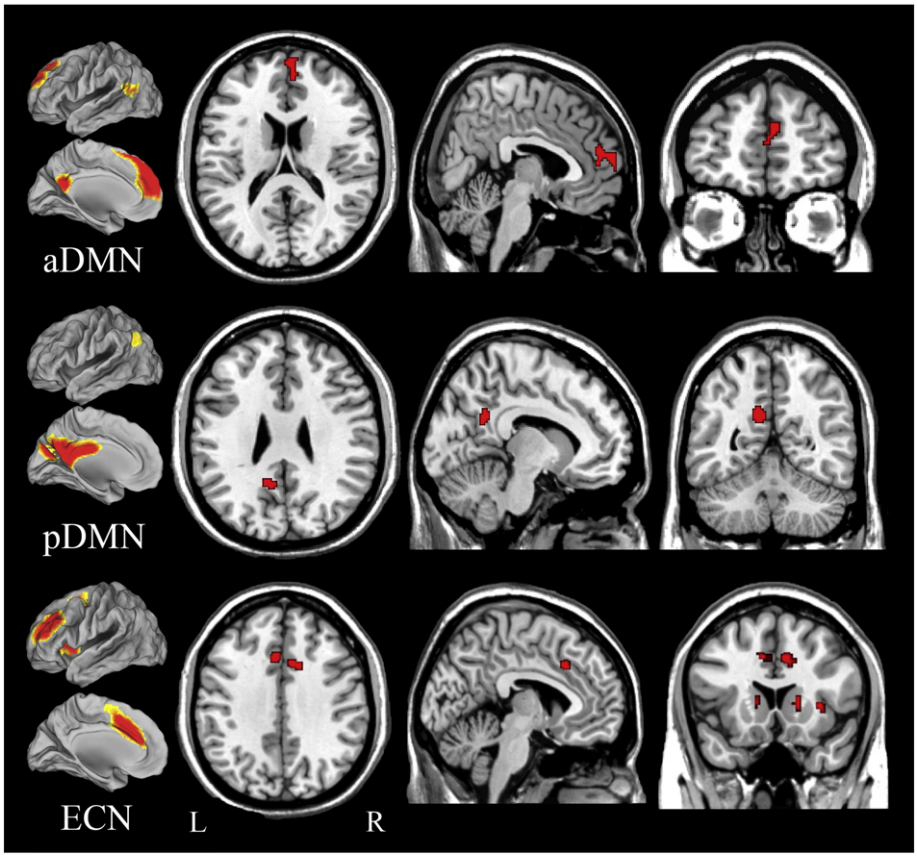

Fig. 2. The differences in synchronization between the two genotype groups. Compared with KIBRA TT individuals, C-carriers showed increased synchronization in the right MPFC of the aDMN, the left PCC of the pDMN, right AI, bilateral Cau, bilateral dACC in the ECN ($P<0.05$, corrected). aDMN, anterior default mode network; AI, anterior insula; Cau, caudate nuclei; dACC, dorsal anterior cingulate cortex; ECN, executive control network; L, left; MPFC, medial prefrontal cortex; PCC, posterior cingulate cortex; pDMN, posterior default mode network; and R, right.

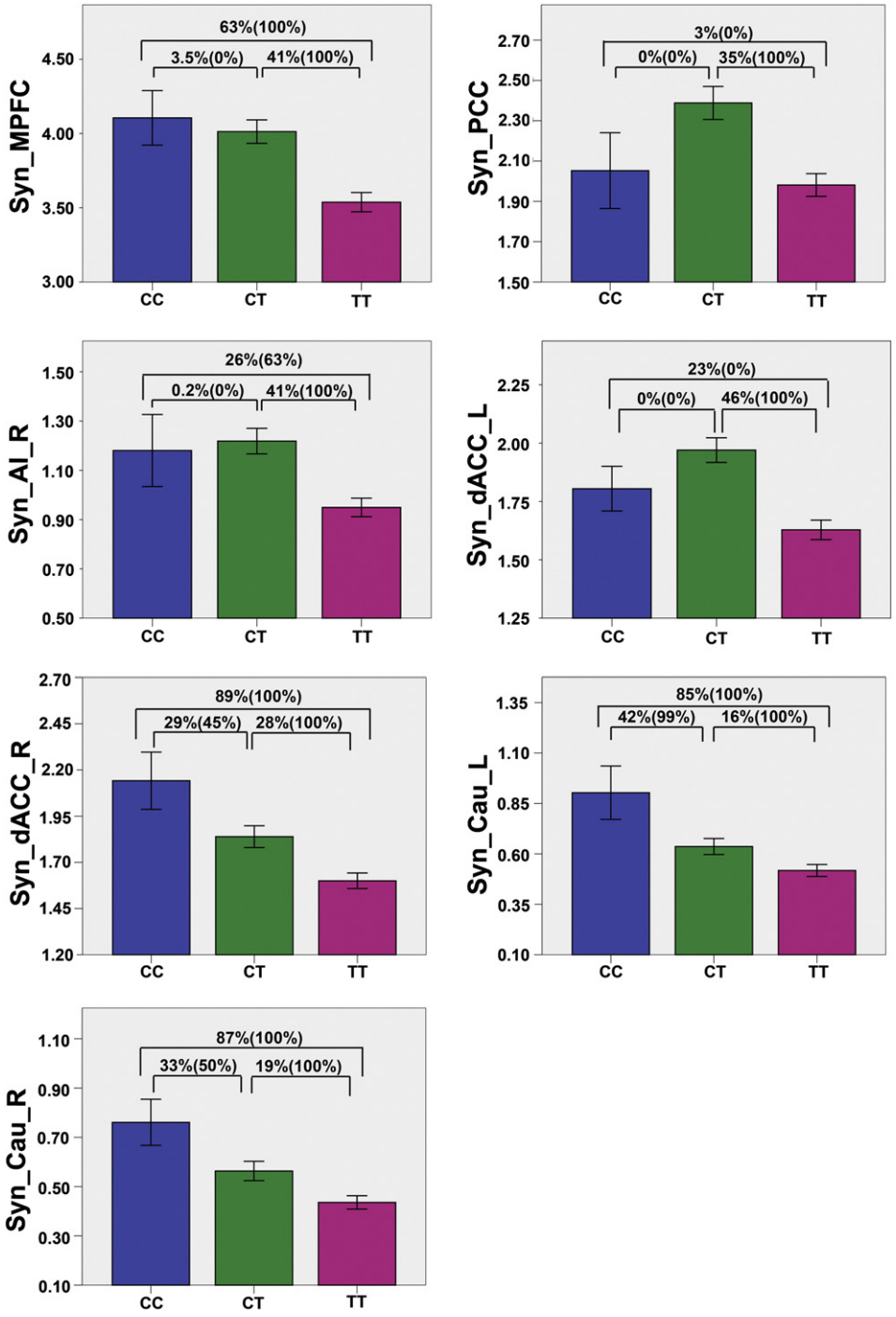

Fig. 3. Results of the percentage of permutation and leave-one-out analyses (shown in parentheses) with significant difference in synchronization of each ROI ($P<0.05$). AI, anterior insula; Cau, caudate nuclei; dACC, dorsal anterior cingulate cortex; L, left; MPFC, medial prefrontal cortex; PCC, posterior cingulate cortex; R, right; and Syn, synchronization.

voxel-based analysis of fractional anisotropy from diffusion tensor imaging data (for detailed methods see supplementary materials). However, we did not find any significant ($P<0.001$, uncorrected) differences in white matter volume and white matter integrity between the two genotypes, suggesting that the KIBRA polymorphism does not significantly affect brain white matter. These findings are consistent with the temporal and spatial expression of KIBRA, which is mainly expressed in the cortex and several memory-related structures such as the hippocampus, temporal lobe, and frontal lobe (Johannsen et al., 2008).

Discussion

KIBRA and episodic memory

The association between a polymorphism in the KIBRA gene and episodic memory has been investigated in 22 independent cohorts (Table S1). Twelve showed a beneficial effect of the T-allele (CT + TT) on episodic memory (Almeida et al., 2008; Bates et al., 2009; Kauppi et al., 2011; Papassotiropoulos et al., 2006; Preuschhof et al., 2010; Schaper

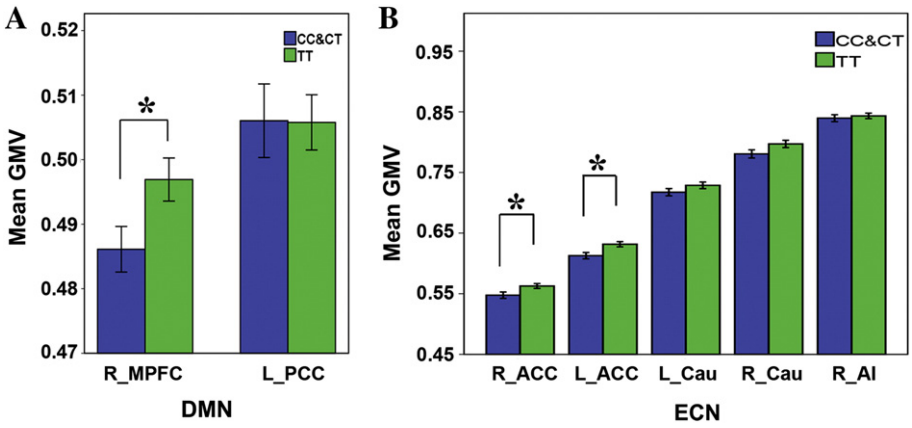

Fig. 4. The GMV differences between KIBRA TT and C-carriers in the DMN and ECN. Compared with the TT individuals, the C-carriers have significantly smaller GMV in the right MPFC of DMN and bilateral dACC of ECN. There is no significant difference in GMV in the left PCC, and a trend that the C-carriers have smaller GMV in the right AI and bilateral Cau. AI, anterior insula; Cau, caudate nuclei; dACC, dorsal anterior cingulate cortex; DMN, default mode network; ECN, executive control network; L, left; MPFC, medial prefrontal cortex; PCC, posterior cingulate cortex; and R, right.

et al., 2008; Vassos et al., 2010; Yasuda et al., 2010), suggesting a protective role of the KIBRA T-allele (Burgess et al., 2011). However, a beneficial effect of the T-allele was not shown in 7/22 cohorts (Bates et al., 2009; Burgess et al., 2011; Jacobsen et al., 2009; Need et al., 2008; Wersching et al., 2011). Moreover, two previous studies even reported a deleterious effect of the T-allele on episodic memory (Nacmias et al., 2008; Wagner et al., 2012). Although the inconsistencies across studies may be related to the differences in age, ethnicity, disease status, and memory tests used in these previous studies, a meta-analysis of 8000 subjects suggested that the KIBRA polymorphism only plays a modest role in episodic memory (Burgess et al., 2011). In contrast to 21/22 cohorts that grouped subjects into CC and T-allele (CT + TT) groups, one study of Japanese patients with AD grouped subjects into TT and C-allele (CC + CT) groups, revealing that C-allele carriers scored lower than TT carriers on tests of episodic memory (Hayashi et al., 2010). Although we did not find a significant difference in memory scores between the C-allele and TT carriers, there was a trend towards poorer memory scores in CC carriers compared to CT and TT carriers. It seems that CC carriers score lower on memory tests; however, there is not enough evidence to show a difference in memory scores between CT and TT carriers. The latter suggests that either the T allele is dominant for better memory scores or the behavioral phenotype is not sensitive enough to show a difference between the CT and TT carriers.

KIBRA and executive function

The association of the polymorphism in the KIBRA gene with executive function is more complex than with episodic memory (Table S2). Although 7/9 independent cohorts did not reveal any significant differences between genotypes (Nacmias et al., 2008; Papassotiropoulos et al., 2006; Preuschhof et al., 2010; Schaper et al., 2008; Wagner et al., 2012; Zhang et al., 2009a), one study on European Americans reported poorer performance in executive function in T-allele carriers, an effect that was modulated by recent tobacco use (Zhang et al., 2009a). Moreover, although there was no main effect of the KIBRA polymorphism on executive function, one study revealed that T-allele carriers with arterial hypertension performed significantly poorer on tests of executive function than non-T-allele carriers (Wersching et al., 2011). In the present study, similar to most previous studies, we did not find a significant difference in executive function between the genotype groups, although there was a trend towards a significant difference in that CC carriers had poorer executive function than CT and TT carriers. These findings demonstrate the complexity of the effect of the KIBRA polymorphism on executive function.

KIBRA and AD

Gene expression studies have demonstrated that KIBRA is highly expressed in memory-related brain regions, including the hippocampus, temporal, frontal and parietal lobes (Johannsen et al., 2008; Papassotiropoulos et al., 2006), which are impaired in AD patients. The association between the KIBRA polymorphism and the risk for AD has been investigated in 6 independent cohorts (Table S3): four have linked KIBRA C-allele homozygote to an increased risk for AD (Burgess et al., 2011; Corneveaux et al., 2010); one study linked the KIBRA T-allele to greater risk for very-late-onset (after the age of 86 years) AD (Rodriguez-Rodriguez et al., 2009); and another study of Japanese subjects did not show any association between the KIBRA polymorphism and the risk for AD (Hayashi et al., 2010). A meta-analysis of more than 8000 subjects showed that the KIBRA T-allele is linked to a decreased risk for AD (Burgess et al., 2011). Differences in age, ethnicity, and AD subtypes may be responsible for the discrepancies across these studies. Evidence for an association between the KIBRA polymorphism and the risk for AD is far from reaching the level of evidence that has been demonstrated for the APOE epsilon.

KIBRA and DMN

The DMN has been extensively associated with episodic memory (Daselaar et al., 2004; Greicius et al., 2004; Otten and Rugg, 2001; Wagner et al., 2005; Wheeler and Buckner, 2003). AD, which is clinically characterized by severe episodic memory impairment, has been associated with structural and functional deficits in the DMN (Greicius et al., 2004; Sorg et al., 2007; Wang et al., 2007; Zhang et al., 2009b). Synchronization of a brain region with its belonging RSN represents the temporal coherence in the resting-state low frequency fluctuations of BOLD signals between a brain region and its belonging RSN, such as the PCC and the posterior DMN. This measure can be calculated by ICA. In patients with AD, decreased synchronization of the DMN is a consistent finding (Greicius et al., 2004; Sorg et al., 2007), suggesting functional deficits in the DMN in AD. However, in healthy young (Filippini et al., 2009) and old individuals (Westlye et al., 2011), APOE 4 carriers with increased genetic risk for AD showed increased synchronization in the DMN compared to non-carriers, which is likely a reflection of functional compensation for the genetic deficit. Alternatively, the increased synchronization of the DMN may also represent a functional abnormality. Regardless, the functional implications of the increased synchronization of the RSN should be further studied.

In the present study, we found that KIBRA C-carriers showed an increased synchronization in the MPFC and PCC of the DMN compared to

TT-genotype subjects. An association between the KIBRA polymorphism and the function of the DMN has been found in three previous studies. One fMRI study of healthy young (20–30 years) subjects reported increased activation in the hippocampus, MPFC, and IPL of the DMN in CC subjects compared to T-allele subjects (Papassotiropoulos et al., 2006). However, two other studies of healthy elderly (>50 years) subjects revealed significantly lower glucose metabolism in the PCC/PCu (Corneveaux et al., 2010) and decreased hippocampal activation (Kauppi et al., 2011) in CC carriers. The age-dependent effect of the KIBRA polymorphism on the activation of the DMN suggests that KIBRA C-allele carriers (especially the CC individuals), who are characterized by poor episodic memory performance, will exhibit compensatory changes (increased activation or synchronization) in the DMN when they are young (Papassotiropoulos et al., 2006), and exhibit a dysfunction (decreased metabolism and activation) in the DMN as they age (Corneveaux et al., 2010; Kauppi et al., 2011).

An interesting finding in the present study is that C-carriers simultaneously exhibited a decrease in GMV and an increase in synchronization in the MPFC compared to TT individuals. These findings suggest that the C-carriers exhibited a GMV deficit in the MPFC during young adulthood, and the increased synchronization in the MPFC is likely a reflection of compensation for the structural deficit, developed to maintain relatively normal cognitive performance in these healthy young participants. Similarly, a functional compensatory mechanism has also been used to explain the increased DMN synchronization in healthy young carriers of the APOE ε4-allele (Filippini et al., 2009). Although there was no explanation for the different effects of the KIBRA polymorphism on the GMVs of the anterior and posterior DMNs, several previous studies may partly support our finding. One study reported that patients with amnestic mild cognitive impairment (aMCI) showed decreased functional connectivity in the PCC and MPFC; however, these patients showed decreased GMV only in the MPFC (Gili et al., 2011). This finding suggests that the reduction of GMV in the MPFC occurs at a stage of aMCI before conversion into AD. However, a functional alteration in the PCC can occur much earlier than the GMV changes in this region, which is also supported by the finding of a reduction of metabolism in the PCC without remarkable atrophy in patients with early AD (Chetelat et al., 2008; Villain et al., 2008). Based on both previous findings and ours, we speculate that the KIBRA polymorphism may preferentially modulate the GMV of the MPFC, but these neural mechanisms need to be further investigated.

KIBRA and ECN

The ECN, also known as the salience network (SN), mainly consists of the DLPFC, dACC and AI (Beckmann et al., 2005; Fox et al., 2006; Greicius et al., 2003; Roosendaal et al., 2010; Seeley et al., 2007). The right AI serves to identify salient stimuli from the vast and continuous stream of visual, auditory, tactile and other sensory inputs. Once such a stimulus is detected, the right AI initiates appropriate transient control signals to engage the dACC and prefrontal cortices that mediate attention, working memory and other higher order cognitive processes while disengaging the DMN (Menon and Uddin, 2010). The dACC has been reported to be involved in a variety of executive functions, such as attention control (Crottaz-Herbette and Menon, 2006; Luo et al., 2007; Smith and Jonides, 1999), conflict monitoring (Botvinick et al., 2004; Carter and van Veen, 2007; Carter et al., 1998), error monitoring and detection (Gehring and Fencsik, 2001; Gehring and Knight, 2000; Lorist et al., 2005; Pourtois et al., 2010), and response selection (Awh and Gehring, 1999; Paus, 2001). We found that C-carriers simultaneously exhibited a decrease in GMV and an increase in synchronization in the dACC bilaterally compared to TT individuals, and we also found increased synchronization in the right AI and the bilateral caudate nucleus of the ECN. These findings suggest that the C-carriers exhibited a GMV deficit in the dACC during young adulthood, and the increased synchronization in the ECN is likely a reflection of compensation for this structural deficit, which maintained relatively normal executive function in this group of healthy young participants.

Limitations

The small number of the CC-individuals (14/288) made our grouping method (CC + CT versus TT) different from most previous studies (CC versus TT + CT), which prevents us from directly comparing our results with previous findings. As described in the Results section, synchronization of all 7 ROIs differed significantly between the CT and TT groups; however, the synchronization of 4/7 ROIs did not differ between the CT and CC groups (Fig. 3). These findings suggest that the combination of the CC and CT is more reasonable at least in the Chinese population. Notably, several non-genetic factors such as smoking and arterial hypertension were not controlled for in this study, which may also impact cognitive function.

Conclusion

KIBRA C-allele carriers exhibited increased synchronization and reduced GMV in the DMN and ECN compared to individuals with the TT genotype, but not in several control networks. The increased synchronization in the DMN and ECN is likely a reflection of compensation for the GMV deficit in these networks in young healthy subjects. Longitudinal studies are required to clarify the role of the DMN and ECN in mediating the association between KIBRA polymorphism and cognitive function.

Acknowledgments

This work was supported by grants from the National Basic Research Program of China (973 program, No. 2011CB707800), the Natural Science Foundation of China (Nos. 81271551 and 81061120533), and the Natural Science Foundation of Tianjin (No. 11JCZDJC19300).

Appendix A. Supplementary data

Supplementary data to this article can be found online at http://dx.doi.org/10.1016/j.neuroimage.2012.12.022.

References

Almeida, O.P., Schwab, S.G., Lautenschlager, N.T., Morar, B., Greenop, K.R., Flicker, L., Wildenauer, D., 2008. KIBRA genetic polymorphism influences episodic memory in later life, but does not increase the risk of mild cognitive impairment. J. Cell. Mol. Med. 12, 1672–1676.
Ashburner, J., 2007. A fast diffeomorphic image registration algorithm. NeuroImage 38, 95–113.
Ashburner, J., Friston, K.J., 2005. Unified segmentation. NeuroImage 26, 839–851.
Awh, E., Gehring, W.J., 1999. The anterior cingulate cortex lends a hand in response selection. Nat. Neurosci. 2, 853–854.
Bates, T.C., Price, J.F., Harris, S.E., Marioni, R.E., Fowkes, F.G., Stewart, M.C., Murray, G.D., Whalley, L.J., Starr, J.M., Deary, I.J., 2009. Association of KIBRA and memory. Neurosci. Lett. 458, 140–143.
Beckmann, C.F., Smith, S.M., 2005. Tensorial extensions of independent component analysis for multisubject FMRI analysis. NeuroImage 25, 294–311.
Beckmann, C.F., DeLuca, M., Devlin, J.T., Smith, S.M., 2005. Investigations into resting-state connectivity using independent component analysis. Phil. Trans. R. Soc. B Biol. Sci. 360, 1001–1013.
Beckmann, C., Mackay, C., Filippin, N., Smith, S., 2009. Group comparison of resting-state FMRI data using multi-subject ica and dual regression. NeuroImage 47 (Suppl. 1), S39–S41.
Beecham, G.W., Martin, E.R., Li, Y.J., Slifer, M.A., Gilbert, J.R., Haines, J.L., Pericak-Vance, M.A., 2009. Genome-wide association study implicates a chromosome 12 risk locus for late-onset Alzheimer disease. Am. J. Hum. Genet. 84, 35–43.
Botvinick, M.M., Cohen, J.D., Carter, C.S., 2004. Conflict monitoring and anterior cingulate cortex: an update. Trends Cogn. Sci. 8, 539–546.
Buckner, R.L., Andrews-Hanna, J.R., Schacter, D.L., 2008. The brain's default network: anatomy, function, and relevance to disease. Ann. N. Y. Acad. Sci. 1124, 1–38.
Burgess, J.D., Pedraza, O., Graff-Radford, N.R., Hirpa, M., Zou, F., Miles, R., Nguyen, T., Li, M., Lucas, J.A., Ivnik, R.J., Crook, J., Pankratz, V.S., Dickson, D.W., Petersen, R.C.,

Younkin, S.G., Ertekin-Taner, N., 2011. Association of common KIBRA variants with episodic memory and AD risk. Neurobiol. Aging 32 (557), e551–e559.
Calhoun, V.D., Adali, T., Pearlson, G.D., Pekar, J.J., 2001. A method for making group inferences from functional MRI data using independent component analysis. Hum. Brain Mapp. 14, 140–151.
Carter, C.S., van Veen, V., 2007. Anterior cingulate cortex and conflict detection: an update of theory and data. Cogn. Affect Behav. Neurosci. 7, 367–379.
Carter, C.S., Braver, T.S., Barch, D.M., Botvinick, M.M., Noll, D., Cohen, J.D., 1998. Anterior cingulate cortex, error detection, and the online monitoring of performance. Science 280, 747–749.
Chao-Gan, Y., Yu-Feng, Z., 2010. DPARSF: a MATLAB toolbox for "Pipeline" data analysis of resting-state fMRI. Front. Syst. Neurosci. 4, 13.
Chetelat, G., Desgranges, B., Landeau, B., Mezenge, F., Poline, J.B., de la Sayette, V., Viader, F., Eustache, F., Baron, J.C., 2008. Direct voxel-based comparison between grey matter hypometabolism and atrophy in Alzheimer's disease. Brain 131, 60–71.
Collignon, A., Maes, F., Delaere, D., Vandermeulen, D., Suetens, P., Marchal, G., 1995. Automated Multi-modality Image Registration Based on Information Theory. Kluwer Academic Publishers, Dordrecht (The Netherlands).
Corneveaux, J.J., Liang, W.S., Reiman, E.M., Webster, J.A., Myers, A.J., Zismann, V.L., Joshipura, K.D., Pearson, J.V., Hu-Lince, D., Craig, D.W., Coon, K.D., Dunckley, T., Bandy, D., Lee, W., Chen, K., Beach, T.G., Mastroeni, D., Grover, A., Ravid, R., Sando, S.B., Aasly, J.O., Heun, R., Jessen, F., Kolsch, H., Rogers, J., Hutton, M.L., Melquist, S., Petersen, R.C., Alexander, G.E., Caselli, R.J., Papassotiropoulos, A., Stephan, D.A., Huentelman, M.J., 2010. Evidence for an association between KIBRA and late-onset Alzheimer's disease. Neurobiol. Aging 31, 901–909.
Crottaz-Herbette, S., Menon, V., 2006. Where and when the anterior cingulate cortex modulates attentional response: combined fMRI and ERP evidence. J. Cogn. Neurosci. 18, 766–780.
Damoiseaux, J.S., Rombouts, S.A., Barkhof, F., Scheltens, P., Stam, C.J., Smith, S.M., Beckmann, C.F., 2006. Consistent resting-state networks across healthy subjects. Proc. Natl. Acad. Sci. U. S. A. 103, 13848–13853.
Daselaar, S.M., Prince, S.E., Cabeza, R., 2004. When less means more: deactivations during encoding that predict subsequent memory. NeuroImage 23, 921–927.
De Luca, M., Beckmann, C.F., De Stefano, N., Matthews, P.M., Smith, S.M., 2006. fMRI resting state networks define distinct modes of long-distance interactions in the human brain. NeuroImage 29, 1359–1367.
Filippini, N., MacIntosh, B.J., Hough, M.G., Goodwin, G.M., Frisoni, G.B., Smith, S.M., Matthews, P.M., Beckmann, C.F., Mackay, C.E., 2009. Distinct patterns of brain activity in young carriers of the APOE-epsilon4 allele. Proc. Natl. Acad. Sci. U. S. A. 106, 7209–7214.
Fox, M.D., Snyder, A.Z., Vincent, J.L., Corbetta, M., Van Essen, D.C., Raichle, M.E., 2005. The human brain is intrinsically organized into dynamic, anticorrelated functional networks. Proc. Natl. Acad. Sci. U. S. A. 102, 9673–9678.
Fox, M.D., Corbetta, M., Snyder, A.Z., Vincent, J.L., Raichle, M.E., 2006. Spontaneous neuronal activity distinguishes human dorsal and ventral attention systems. Proc. Natl. Acad. Sci. U. S. A. 103, 10046–10051.
Gehring, W.J., Fencsik, D.E., 2001. Functions of the medial frontal cortex in the processing of conflict and errors. J. Neurosci. 21, 9430–9437.
Gehring, W.J., Knight, R.T., 2000. Prefrontal-cingulate interactions in action monitoring. Nat. Neurosci. 3, 516–520.
Gili, T., Cercignani, M., Serra, L., Perri, R., Giove, F., Maraviglia, B., Caltagirone, C., Bozzali, M., 2011. Regional brain atrophy and functional disconnection across Alzheimer's disease evolution. J. Neurol. Neurosurg. Psychiatry 82, 58–66.
Gong, Y., 1989. Manual of Wechsler Memory Scale-China Revised. Hunan Mapping Press, Changsha (China).
Greicius, M.D., Krasnow, B., Reiss, A.L., Menon, V., 2003. Functional connectivity in the resting brain: a network analysis of the default mode hypothesis. Proc. Natl. Acad. Sci. U. S. A. 100, 253–258.
Greicius, M.D., Srivastava, G., Reiss, A.L., Menon, V., 2004. Default-mode network activity distinguishes Alzheimer's disease from healthy aging: evidence from functional MRI. Proc. Natl. Acad. Sci. U. S. A. 101, 4637–4642.
Hayashi, N., Kazui, H., Kamino, K., Tokunaga, H., Takaya, M., Yokokoji, M., Kimura, R., Kito, Y., Wada, T., Nomura, K., Sugiyama, H., Yamamoto, D., Yoshida, T., Currais, A., Soriano, S., Hamasaki, T., Yamamoto, M., Yasuda, Y., Hashimoto, R., Tanimukai, H., Tagami, S., Okochi, M., Tanaka, T., Kudo, T., Morihara, T., Takeda, M., 2010. KIBRA genetic polymorphism influences episodic memory in Alzheimer's disease, but does not show association with disease in a Japanese cohort. Dement. Geriatr. Cogn. Disord. 30, 302–308.
Heaton, R., 1999. Wisconsin Card Sorting Test (Computer Version 3 for Windows Research Edition). Psychological Assessment Resources, Odessa, FL.
Jacobsen, L.K., Picciotto, M.R., Heath, C.J., Mencl, W.E., Gelernter, J., 2009. Allelic variation of calsyntenin 2 (CLSTN2) modulates the impact of developmental tobacco smoke exposure on mnemonic processing in adolescents. Biol. Psychiatry 65, 671–679.
Johannsen, S., Duning, K., Pavenstadt, H., Kremerskothen, J., Boeckers, T.M., 2008. Temporal–spatial expression and novel biochemical properties of the memory-related protein KIBRA. Neuroscience 155, 1165–1173.
Kauppi, K., Nilsson, L.G., Adolfsson, R., Eriksson, E., Nyberg, L., 2011. KIBRA polymorphism is related to enhanced memory and elevated hippocampal processing. J. Neurosci. 31, 14218–14222.
Lorist, M.M., Boksem, M.A., Ridderinkhof, K.R., 2005. Impaired cognitive control and reduced cingulate activity during mental fatigue. Brain Res. Cogn. Brain Res. 24, 199–205.
Luo, Q., Mitchell, D., Jones, M., Mondillo, K., Vythilingam, M., Blair, R.J., 2007. Common regions of dorsal anterior cingulate and prefrontal–parietal cortices provide attentional control of distracters varying in emotionality and visibility. NeuroImage 38, 631–639.
Mantini, D., Perrucci, M.G., Del Gratta, C., Romani, G.L., Corbetta, M., 2007. Electrophysiological signatures of resting state networks in the human brain. Proc. Natl. Acad. Sci. U. S. A. 104, 13170–13175.
Menon, V., Uddin, L.Q., 2010. Saliency, switching, attention and control: a network model of insula function. Brain Struct. Funct. 214, 655–667.
Nacmias, B., Bessi, V., Bagnoli, S., Tedde, A., Cellini, E., Piccini, C., Sorbi, S., Bracco, L., 2008. KIBRA gene variants are associated with episodic memory performance in subjective memory complaints. Neurosci. Lett. 436, 145–147.
Need, A.C., Attix, D.K., McEvoy, J.M., Cirulli, E.T., Linney, K.N., Wagoner, A.P., Gumbs, C.E., Giegling, I., Moller, H.J., Francks, C., Muglia, P., Roses, A., Gibson, G., Weale, M.E., Rujescu, D., Goldstein, D.B., 2008. Failure to replicate effect of Kibra on human memory in two large cohorts of European origin. Am. J. Med. Genet. B Neuropsychiatr. Genet. 147B, 667–668.
Otten, L.J., Rugg, M.D., 2001. When more means less: neural activity related to unsuccessful memory encoding. Curr. Biol. 11, 1528–1530.
Papassotiropoulos, A., Stephan, D.A., Huentelman, M.J., Hoerndli, F.J., Craig, D.W., Pearson, J.V., Huynh, K.D., Brunner, F., Corneveaux, J., Osborne, D., Wollmer, M.A., Aerni, A., Coluccia, D., Hanggi, J., Mondadori, C.R., Buchmann, A., Reiman, E.M., Caselli, R.J., Henke, K., de Quervain, D.J., 2006. Common Kibra alleles are associated with human memory performance. Science 314, 475–478.
Paus, T., 2001. Primate anterior cingulate cortex: where motor control, drive and cognition interface. Nat. Rev. Neurosci. 2, 417–424.
Pourtois, G., Vocat, R., N'Diaye, K., Spinelli, L., Seeck, M., Vuilleumier, P., 2010. Errors recruit both cognitive and emotional monitoring systems: simultaneous intracranial recordings in the dorsal anterior cingulate gyrus and amygdala combined with fMRI. Neuropsychologia 48, 1144–1159.
Preuschhof, C., Heekeren, H.R., Li, S.C., Sander, T., Lindenberger, U., Backman, L., 2010. KIBRA and CLSTN2 polymorphisms exert interactive effects on human episodic memory. Neuropsychologia 48, 402–408.
Raichle, M.E., MacLeod, A.M., Snyder, A.Z., Powers, W.J., Gusnard, D.A., Shulman, G.L., 2001. A default mode of brain function. Proc. Natl. Acad. Sci. U. S. A. 98, 676–682.
Rodriguez-Rodriguez, E., Infante, J., Llorca, J., Mateo, I., Sanchez-Quintana, C., Garcia-Gorostiaga, I., Sanchez-Juan, P., Berciano, J., Combarros, O., 2009. Age-dependent association of KIBRA genetic variation and Alzheimer's disease risk. Neurobiol. Aging 30, 322–324.
Roosendaal, S.D., Schoonheim, M.M., Hulst, H.E., Sanz-Arigita, E.J., Smith, S.M., Geurts, J.J., Barkhof, F., 2010. Resting state networks change in clinically isolated syndrome. Brain 133, 1612–1621.
Schacter, D.L., Addis, D.R., Buckner, R.L., 2007. Remembering the past to imagine the future: the prospective brain. Nat. Rev. Neurosci. 8, 657–661.
Schaper, K., Kolsch, H., Popp, J., Wagner, M., Jessen, F., 2008. KIBRA gene variants are associated with episodic memory in healthy elderly. Neurobiol. Aging 29, 1123–1125.
Seeley, W.W., Menon, V., Schatzberg, A.F., Keller, J., Glover, G.H., Kenna, H., Reiss, A.L., Greicius, M.D., 2007. Dissociable intrinsic connectivity networks for salience processing and executive control. J. Neurosci. 27, 2349–2356.
Smith, E.E., Jonides, J., 1999. Storage and executive processes in the frontal lobes. Science 283, 1657–1661.
Smith, S.M., Jenkinson, M., Woolrich, M.W., Beckmann, C.F., Behrens, T.E.J., Johansen-Berg, H., Bannister, P.R., De Luca, M., Drobnjak, I., Flitney, D.E., Niazy, R.K., Saunders, J., Vickers, J., Zhang, Y.Y., De Stefano, N., Brady, J.M., Matthews, P.M., 2004. Advances in functional and structural MR image analysis and implementation as FSL. NeuroImage 23, S208–S219.
Sorg, C., Riedl, V., Muhlau, M., Calhoun, V.D., Eichele, T., Laer, L., Drzezga, A., Forstl, H., Kurz, A., Zimmer, C., Wohlschlager, A.M., 2007. Selective changes of resting-state networks in individuals at risk for Alzheimer's disease. Proc. Natl. Acad. Sci. U. S. A. 104, 18760–18765.
Spreng, R.N., Mar, R.A., Kim, A.S., 2009. The common neural basis of autobiographical memory, prospection, navigation, theory of mind, and the default mode: a quantitative meta-analysis. J. Cogn. Neurosci. 21, 489–510.
Svoboda, E., McKinnon, M.C., Levine, B., 2006. The functional neuroanatomy of autobiographical memory: a meta-analysis. Neuropsychologia 44, 2189–2208.
Thomas, G., Sinville, R., Sutton, S., Farquar, H., Hammer, R.P., Soper, S.A., Cheng, Y.W., Barany, F., 2004. Capillary and microelectrophoretic separations of ligase detection reaction products produced from low-abundant point mutations in genomic DNA. Electrophoresis 25, 1668–1677.
Vassos, E., Bramon, E., Picchioni, M., Walshe, M., Filbey, F.M., Kravariti, E., McDonald, C., Murray, R.M., Collier, D.A., Toulopoulou, T., 2010. Evidence of association of KIBRA genotype with episodic memory in families of psychotic patients and controls. J. Psychiatr. Res. 44, 795–798.
Villain, N., Desgranges, B., Viader, F., de la Sayette, V., Mezenge, F., Landeau, B., Baron, J.C., Eustache, F., Chetelat, G., 2008. Relationships between hippocampal atrophy, white matter disruption, and gray matter hypometabolism in Alzheimer's disease. J. Neurosci. 28, 6174–6181.
Wagner, A.D., Shannon, B.J., Kahn, I., Buckner, R.L., 2005. Parietal lobe contributions to episodic memory retrieval. Trends Cogn. Sci. 9, 445–453.
Wagner, A.K.A.P., Hatz, L.E., Scanlon, J.M., Niyonkuru, C., Miller, M.A., Ricker, J.H., Conley, Y.P., Ferrell, R.E., 2012. Association of KIBRA rs17070145 polymorphism and episodic memory in individuals with severe TBI. Brain Inj. (Epub ahead of print).
Wang, K., Liang, M., Wang, L., Tian, L., Zhang, X., Li, K., Jiang, T., 2007. Altered functional connectivity in early Alzheimer's disease: a resting-state fMRI study. Hum. Brain Mapp. 28, 967–978.
Wersching, H., Guske, K., Hasenkamp, S., Hagedorn, C., Schiwek, S., Jansen, S., Witte, V., Wellmann, J., Lohmann, H., Duning, K., Kremerskothen, J., Knecht, S., Brand, E., Floel, A., 2011. Impact of common KIBRA allele on human cognitive functions. Neuropsychopharmacology 36, 1296–1304.

Westlye, E.T., Lundervold, A., Rootwelt, H., Lundervold, A.J., Westlye, L.T., 2011. Increased hippocampal default mode synchronization during rest in middle-aged and elderly APOE epsilon4 carriers: relationships with memory performance. J. Neurosci. 31, 7775–7783.

Wheeler, M.E., Buckner, R.L., 2003. Functional dissociation among components of remembering: control, perceived oldness, and content. J. Neurosci. 23, 3869–3880.

Yasuda, Y., Hashimoto, R., Ohi, K., Fukumoto, M., Takamura, H., Iike, N., Yoshida, T., Hayashi, N., Takahashi, H., Yamamori, H., Morihara, T., Tagami, S., Okochi, M., Tanaka, T., Kudo, T., Kamino, K., Ishii, R., Iwase, M., Kazui, H., Takeda, M., 2010. Association study of KIBRA gene with memory performance in a Japanese population. World J. Biol. Psychiatry 11, 852–857.

Yi, P., Chen, Z., Zhao, Y., Guo, J., Fu, H., Zhou, Y., Yu, L., Li, L., 2009. PCR/LDR/capillary electrophoresis for detection of single-nucleotide differences between fetal and maternal DNA in maternal plasma. Prenat. Diagn. 29, 217–222.

Zhang, H., Kranzler, H.R., Poling, J., Gruen, J.R., Gelernter, J., 2009a. Cognitive flexibility is associated with KIBRA variant and modulated by recent tobacco use. Neuropsychopharmacology 34, 2508–2516.

Zhang, H.Y., Wang, S.J., Xing, J., Liu, B., Ma, Z.L., Yang, M., Zhang, Z.J., Teng, G.J., 2009b. Detection of PCC functional connectivity characteristics in resting-state fMRI in mild Alzheimer's disease. Behav. Brain Res. 197, 103–108.

Zhang, H., Zuo, X.N., Ma, S.Y., Zang, Y.F., Milham, M.P., Zhu, C.Z., 2010. Subject order-independent group ICA (SOI-GICA) for functional MRI data analysis. NeuroImage 51, 1414–1424.